

## Accepted Manuscript

### Template Directed Synthesis of Half Condensed Schiff Base Complexes of Cu(II) and Co(III) : Structural and Magnetic Studies

Priyanka Pandey, Abhineet Verma, Kateryna Bretosh, Jean-Pascal Sutter, Sailaja S. Sunkari

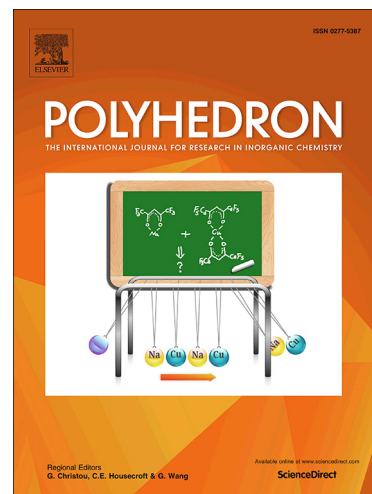
PII: S0277-5387(19)30138-X  
DOI: <https://doi.org/10.1016/j.poly.2019.02.037>  
Reference: POLY 13781

To appear in: *Polyhedron*

Received Date: 5 December 2018  
Revised Date: 14 February 2019  
Accepted Date: 15 February 2019

Please cite this article as: P. Pandey, A. Verma, K. Bretosh, J-P. Sutter, S.S. Sunkari, Template Directed Synthesis of Half Condensed Schiff Base Complexes of Cu(II) and Co(III) : Structural and Magnetic Studies, *Polyhedron* (2019), doi: <https://doi.org/10.1016/j.poly.2019.02.037>

This is a PDF file of an unedited manuscript that has been accepted for publication. As a service to our customers we are providing this early version of the manuscript. The manuscript will undergo copyediting, typesetting, and review of the resulting proof before it is published in its final form. Please note that during the production process errors may be discovered which could affect the content, and all legal disclaimers that apply to the journal pertain.



# Template Directed Synthesis of Half Condensed Schiff Base Complexes of Cu(II) and Co(III) : Structural and Magnetic Studies

Priyanka Pandey,<sup>a</sup> Abhineet Verma,<sup>a</sup> Kateryna Bretosh,<sup>b</sup> Jean-Pascal Sutter<sup>b</sup> and Sailaja S.

Sunkari<sup>\*,a</sup>

<sup>a</sup>Department of Chemistry, Mahila Mahavidyalay, Banaras Hindu University, Varanasi 221 005, India

<sup>b</sup>LCC-CNRS, Université de Toulouse, CNRS, Toulouse, France

## Abstract

By the proper choice of the substituents on the aldehyde and amine groups, the nature of the Schiff base formed (fully condensed or half condensed) can be tuned by the templating effect of the metal ion. The condensation of 5-chlorosalicylaldehyde with ethylene diamine in the presence of Co(II) or Cu(II) cations and azido anions has afforded two new half condensed Schiff base metal complexes  $[\text{CuL}(\mu\text{-}1,1\text{-N}_3)]_2$  (**1**) and  $[\text{CoL}_2]\text{N}_3\cdot\text{H}_2\text{O}$  (**2**), where L = (E)-2-((2-aminoethyl)methyl)-4-chlorophenol, that were structurally characterized by X-ray analysis, IR and UV spectra. Complex **1** is an asymmetric  $\mu\text{-}1,1$  azide bridged dimer displaying weak antiferromagnetic interactions ( $J = -2.93 \pm 0.03 \text{ cm}^{-1}$ ), in agreement with the axial-equatorial  $\text{N}_3\text{-}$  linkage between the two copper centers. Complex **2** is a monomer of a low spin Co(III) ion.

## 1. Introduction

The synthesis and structural studies of polynuclear metal complexes is well known in coordination chemistry due to their possible applications in catalysis,<sup>[1]</sup> molecule based magnetism,<sup>[2]</sup> sensing,<sup>[3]</sup> DNA cleavage<sup>[4]</sup> and so on. Among the several types of ligands used, Schiff bases (SBs) are unique with their planar geometry providing four or three coordination sites depending on the type of condensation product, viz. a fully condensed SB or a half condensed SB.<sup>[5]</sup> The planarity imposed by the fully condensed Schiff base ligands is well suited for encapsulating metal ions into the cavity of the ligating phenoxo oxygen and imino nitrogen atoms, there by leaving the axial positions of a typical metal ion with an octahedral geometry

free, allowing for coordination to other ligating species. Depending on the synthetic conditions as well as the geometry and ligating characteristics of the auxiliary ligands, such attempts led to the formation of discrete<sup>[6]</sup> or polymeric/network structures.<sup>[7]</sup> A close look at the reported Schiff base complexes reveals that the formation of a fully or half condensed Schiff base appears to be directed by the symmetry of the amine,<sup>[8]</sup> nature of substituents on the amino N atom,<sup>[9]</sup> orientation of the amino group with respect to the substituent groups present on the carbon atom to which the amino N atom is attached<sup>[10]</sup> and the variations in the donor capability of the N lone pair due to its involvement in conjugation with available double bonds.<sup>[11]</sup> Irrespective of the molar ratios, a conformational free symmetric amine, having bulky groups that restrict the free rotation of the amino group, leads to a fully condensed Schiff base that may be isolated. In the absence of the conditions that lead to a fully condensed Schiff base, as described above, isolation of a half condensed Schiff base with a symmetric amine is possible only under the templating effect of a metal ion.<sup>[12]</sup> Such isolated complexes of half condensed Schiff bases have been found with Cu(II)<sup>[13]</sup> and Ni(II) ions<sup>[8a,14]</sup> directed by anions like azide, cyanate, thiocyanate and dicyanamide.

In the context of magneto chemistry, the literature is saturated with numerous examples of fully condensed Schiff base metal complexes, especially copper complexes, which help establish magneto structural correlations.<sup>[15]</sup> Among the auxiliary ligands, azides are unique with reference to their bridging modes in Cu(II) complexes, thus generating a plethora of structures of relevance in magneto chemistry.<sup>[16]</sup> Such systems provide ideal test systems for understanding the basics of magnetic interactions in extended systems.<sup>[17]</sup> Previously we have also demonstrated the formation of tetranuclear clusters of Cu(II) ions involving salpn/salophen as the SB and azide as an auxiliary ligand.<sup>[18]</sup> However, a change in the aldehyde component of the Schiff base from a simple aldehyde to one with chloro substitution at the fifth position led to the formation of half condensed Schiff bases templated by the metal ion. The number of half condensed Schiff base complexes are still limited compared to their fully condensed counter parts. Contrary to the fully condensed Schiff base complexes with predefined geometrical constraints, half condensed Schiff base complexes with their tridentate coordination capabilities can generate versatile structures with modified coordination geometries which may be helpful in changing the electronic structure of the metal ion, leading to desired magnetic behavior, depending on the metal ion, auxiliary ligands and the synthetic conditions. Sparsely reported examples include Fe(III) complexes of

halogenated quinolyl salicylaldimines with  $\text{SCN}^{-[19]}$  and pseudo halide bridged dinuclear copper(II) complexes with naphthaldehyde and substituted diamines<sup>[20]</sup> Highlighting the potential of half condensed Schiff base complexes in generating structurally rich systems of magnetic relevance and a means to deliberately synthesize them, herein we report the synthesis and structures of Cu(II) and Co(III) complexes involving the half condensed Schiff base (E)-2-((2-aminoethyl)methyl)-4-chlorophenol (L) and the azide ligand, along with the magnetic properties of the Cu(II) complex **2**.

## 2. Experimental section

### 2.1 Materials and instrumentation

$\text{Cu}(\text{CH}_3\text{COO})_2 \cdot \text{H}_2\text{O}$ ,  $\text{Co}(\text{CH}_3\text{COO})_2 \cdot 4\text{H}_2\text{O}$ , ethylenediamine and 5-chlorosalicylaldehyde were purchased from Sigma Aldrich chemicals. Infrared spectra were recorded on a Perkin Elmer FTIR spectrometer, Spectrum-2 as KBr pellets in the region  $400\text{--}4000\text{ cm}^{-1}$ . Elemental analyses were carried out on a CE-40 elemental analyzer for both complexes. Electronic spectra were recorded on a CARY 100 BIO UV-Visible spectrophotometer. Variable-temperature dc susceptibility measurements were performed on a Quantum Design MPMS-5 SQUID magnetometer. Diamagnetic corrections were applied for the compounds' constituent atoms using Pascal's constants and for the sample holder. The cyclic voltammogram of **2** was recorded with Auto lab (PG STAT, 302, The Netherlands, NOVA 1.11 software) using a conventional three-electrode system.

**Caution:** Azide as well as their metal complexes are potentially explosive and should be handled with great care and in small quantities.

### 2.2 Synthesis

#### 2.2.1. Synthesis of the complexes

2.2.1.1.  $[\text{CuL}(\mu_{1,1}\text{-N}_3)]_2$  (**1**): To 10 mL methanolic solution of 5-chlorosalicylaldehyde (0.328 g, 2.00 mmol), ethylene diamine (80.00  $\mu\text{L}$ , 1.00 mmol) was added dropwise and stirred for 10 minutes. To this solution, a 10 mL methanolic solution of  $\text{Cu}(\text{CH}_3\text{COO})_2 \cdot \text{H}_2\text{O}$  (0.400 g, 2.00 mmol) was added dropwise under stirring, and stirring was continued for 15 minutes, followed by the addition of a 7 mL methanolic solution of  $\text{NaN}_3$  (0.120 g, 2.00 mmol). This mixture was

then refluxed at 60 °C for 3 hours under continuous stirring. X-ray quality crystals were obtained within 6-7 days from slow evaporation of the mother liquor at room temperature (35 °C).

Yield: 0.208 g (67.75 %, 0.68 mmol), M.P. = 273 (±1) °C. Analysis Calculated (found) for  $C_{18}H_{20}N_{10}O_2Cl_2Cu_2$ : C, 35.65 (35.53); H, 3.32 (3.37); N, 23.10 (23.14) %. FT-IR ( $cm^{-1}$ ): 3293(br), 3213(w), 3126(w), 2921(w), 2851(w), 2038(s), 1651(s), 1639(s), 1588(s), 1457(s), 1368(m), 1310(s), 1175(s), 1132(m), 1049(s), 837(s), 704(s), 655(m), 459(m).

2.2.1.2.  $[CoL_2]N_3 \cdot H_2O$  (**2**): To a 7 mL methanolic solution of 5-chlorosalicylaldehyde (0.116 g, 0.74 mmol), ethylene diamine (26.00  $\mu$ L, 0.37 mmol) was added dropwise, resulting in a yellow solution. A 5 mL aqueous solution of  $Co(CH_3COO)_2 \cdot 2H_2O$  (0.093 g, 0.37 mmol) was then added to this solution, dropwise with continuous stirring, resulting in the formation of a brown precipitate, followed by addition of a 5 mL aqueous solution of  $NaN_3$  (0.048 g, 0.74 mmol). The whole contents were transferred to a 25 mL Teflon reactor and heated at 500 °C for 5 hours under autogenous pressure. Subsequently, the vessel was cooled to room temperature. The small amount of precipitate that formed was removed by filtration and the clear blood red filtrate was left at RT (35 °C), from which X-ray quality red block shaped crystals were obtained within 2-3 days.

Yield: 0.140 g (74.20 %, 0.27 mmol), M.P. = 241 (±1) °C. Analysis Calculated (found) for  $C_{18}H_{18}N_7O_3Cl_2Co$ : C, 42.37 (42.53); H, 3.56 (3.47); N, 19.22 (19.14) %. FT-IR ( $cm^{-1}$ ): 3197(br), 3102(w), 2956(w), 2922(w), 2036(s), 1646(s), 1596(s), 1460(s), 1375(m), 1306(s), 1148(m), 1133(s), 1064(s), 830(m), 702(s), 628(m), 484(m).

### 2.3. X-ray crystallography

Crystal data for complex **1** were collected on a Saturn 724 (4x4 bin mode) at 77 K and for **2** on a Bruker APEX-II CCD diffractometer using graphite monochromatized Mo K $\alpha$  radiation at 298 K ( $\lambda = 0.71073$  Å). The data of **1** were reduced using CrystalClear (Rigaku/MSI Inc., 2006) and for complex **2** using Bruker SAINT. The structures were solved by direct methods and refined by full matrix least squares on  $F^2$  using SHELX-2016.<sup>[21]</sup> The non-hydrogen atoms were refined with anisotropic thermal parameters. All the ring hydrogen atoms were geometrically fixed and allowed to refine using a riding model. Water hydrogen atoms for **2** were located from difference maps and their positions refined by DFIX, while thermal parameters were refined using a riding

model. The refinement converged to a final  $R1 = 0.0260$ ;  $wR2 = 0.0664$  for **1** and  $wR2 = 0.0353$ ,  $wR2 = 0.0972$  for **2**. Important crystal data are presented in Table 1 and selected inter-atomic distances and angles in Table 2. Drawings were made using ORTEP-III<sup>[22]</sup> and Mercury.<sup>[23]</sup>

**Table 1.** Important Crystallographic data for complexes **1** and **2**.

	<b>1</b>	<b>2</b>
Formula	$C_{18}H_{20}N_{10}O_2Cl_2Cu_2$	$C_{18}H_{18}N_7O_3Cl_2Co$
Fw	303.21	510.22
Crystal system	Triclinic	Monoclinic
Space group	$P\bar{1}$	$P2_1/c$
$a$ (Å)	5.7113(19)	9.8998(4)
$b$ (Å)	8.463(3)	22.2831(10)
$c$ (Å)	11.860(4)	10.4143(5)
$\alpha$ (°)	77.118(7)	90
$\beta$ (°)	86.469(11)	114.507(1)
$\gamma$ (°)	80.549(10)	90
$V$ (Å <sup>3</sup> )	551.1(3)	2090.41(16)
$Z$	2	4
$F(000)$	306	1040
$\mu$ (mm <sup>-1</sup> )	2.213	1.113
$\rho$ (g cm <sup>-3</sup> )	1.827	1.621
$R_{int}$	0.0311	0.0449
$R$ [ $I > 2\sigma(I)$ ]	0.0260	0.0353
$wR2$ [ $I > 2\sigma(I)$ ]	0.0664	0.0972
$R$ (all data)	0.0313	0.0413
$wR2$ (all data)	0.0680	0.1006
GoF	1.009	1.076
$\lambda$ (Å)	0.71073	0.71073

$$R1 = \sum ||F_o| - |F_c|| / \sum |F_o|; wR2 = [\sum w(|F_o|^2 - |F_c|^2)^2 / \sum w|F_o|^2]^{1/2}.$$

## 2.4. Hirshfeld surface analysis

Molecular Hirshfeld surfaces in the crystal structure were examined on the basis of the electron distribution, calculated as the sum of the spherical atom electron densities. The Hirshfeld surfaces were mapped with  $d_{\text{norm}}$ , the normalized contact distance based on both  $d_e$  (the distance from the point to the nearest nucleus external to the surface) and  $d_i$  (the distance to the nearest nucleus internal to the surface) and the van der Waals (vdW) radii of the atom, given by equation (1). The value of  $d_{\text{norm}}$  is negative or positive depending on the intermolecular contacts being shorter or longer than the van der Waals separations. The Hirshfeld surface and associated 2D fingerprint plots were calculated using CrystalExplorer 2.1.30.<sup>[24]</sup> The 2D plots were created by binning ( $d_e$ ,  $d_i$ ) pairs in intervals of 0.01 Å and coloring each bin (essentially a pixel) of the resulting 2D histogram, as a function of the fraction of surface points in that bin, ranging from blue (few points) through green to red (many points). Graphical plots of the molecular Hirshfeld surfaces were mapped with  $d_{\text{norm}}$  using a red–white–blue color scheme, where red highlights shorter contacts, white for contacts around the vdW separation and blue for longer contacts.

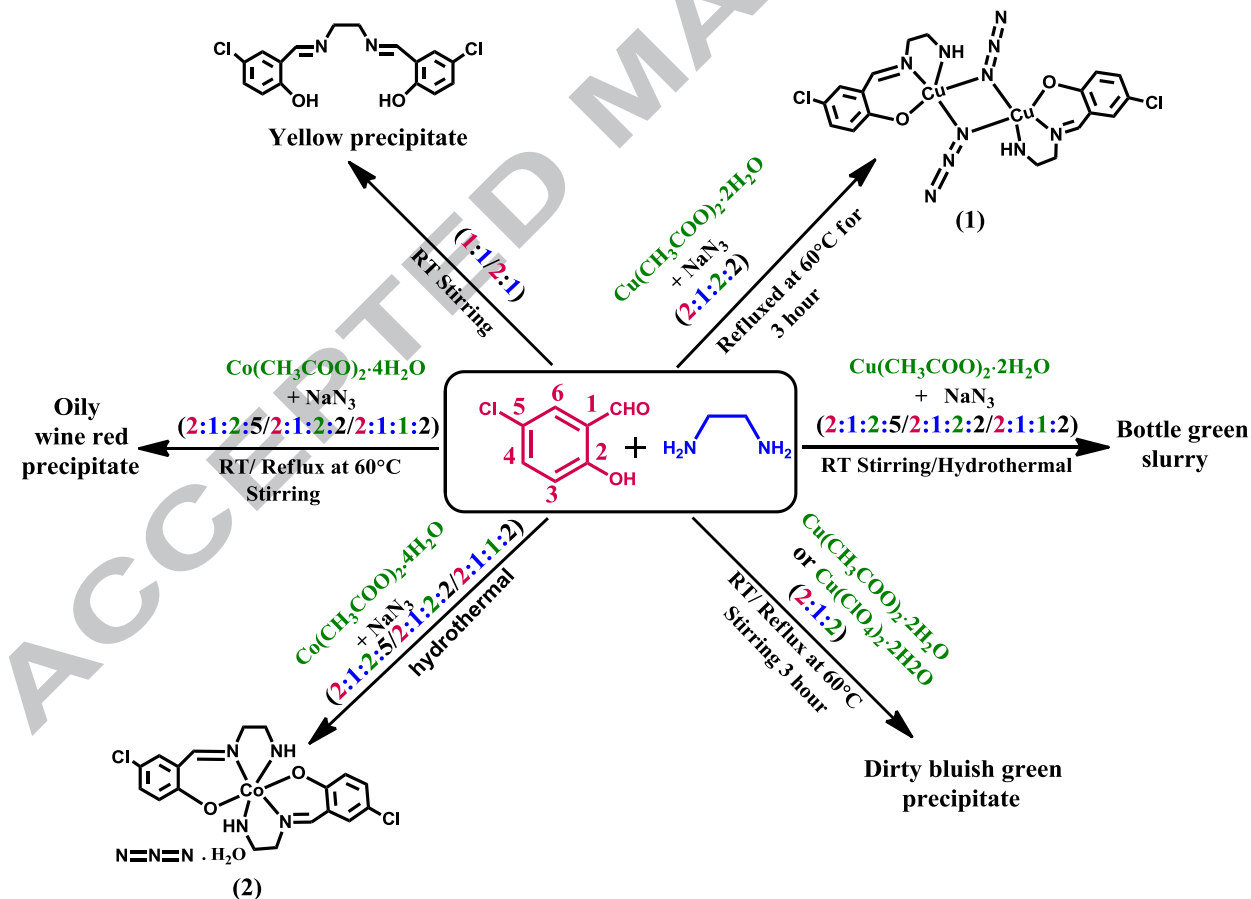
$$d_{\text{norm}} = [(d_i - r_i^{\text{vdW}}) / r_i^{\text{vdW}}] + [(d_e - r_e^{\text{vdW}}) / r_e^{\text{vdW}}] \quad (1)$$

## 3. Results and discussion

### 3.1. Synthesis and IR spectra

Both complexes **1** and **2** were obtained in moderately good yields by the self assembly of the aldehyde, amine, metal and anion in 2:1:2:2 molar ratios, without prior isolation of the ligand. However, reacting only the amine and aldehyde in either 1:1 or 1:2 ratios always yielded a fully condensed Schiff base (Scheme 1). In both complexes, the half condensed Schiff base product was obtained, in spite of the available molar ratios of the aldehyde and amine for the formation of a fully condensed Schiff base. This may be attributed to the templating effect of the metal ion directed by the azide ligand, which stabilizes a square pyramidal copper complex with three coordinating sites occupied by the half condensed Schiff base and the remaining two sites by the asymmetrically bridging azide ligand. Several such half condensed Schiff base complexes of copper with azide, cyanate and thiocyanate ligands were also reported previously by reacting the aldehyde and amine in a 1:1 molar ratio.<sup>[25]</sup> However, we have not come across any reports of half condensed Schiff bases, despite the available molar ratios of 1:2 for amine and aldehydes.

Complex **1** was formed under reflux at 60 °C and **2** under hydrothermal conditions. In the case of **1**, refluxing the solution yielded crystals from the mother liquor. If not refluxed, a highly insoluble precipitate forms by room temperature stirring of the components which could not be further crystallized. Reaction with the preformed Schiff base, Cu(II) ions and azide, either by simple stirring or refluxing, also yields a green slurry which could not be characterized further. In the case of **2**, a gel-like precipitate formation takes place at either room temperature stirring or under reflux conditions. Only heating under pressure afforded crystals of compound **2**. Further, it has been observed that varying the aldehyde, amine, metal and anion molar ratios from 2:1:1:1/2:1:1:2/2:1:2:2/2:1:2:5 always afforded only **2**; while in the case of **1**, variation of aldehyde, amine, metal and anion ratios from 2:1:2:2 to 2:1:1:1/2:1:1:2/2:1:2:5 resulted in dirty green slurry formation which could not be further crystallized. Scheme 1 summarizes the reaction conditions and products formed.



**Scheme 1:** Summary of the synthetic conditions favoring formation of **1** and **2**.

The IR spectra of the complexes show absorption peaks in the range 3293-2851  $\text{cm}^{-1}$  which are assigned to  $\nu_{\text{as}}(\text{N-H})$  of the Schiff base, indicating the presence of an amine group (Figure S1). The imine ( $\text{C}=\text{N}$ ) stretching frequency occurs between 1645 to 1655  $\text{cm}^{-1}$ , while peaks at 2038  $\text{cm}^{-1}$  correspond to the  $\mu$ -1,1 bridging mode of the azido anions and peaks at 2086  $\text{cm}^{-1}$  corresponds to the free azide.<sup>[26]</sup>

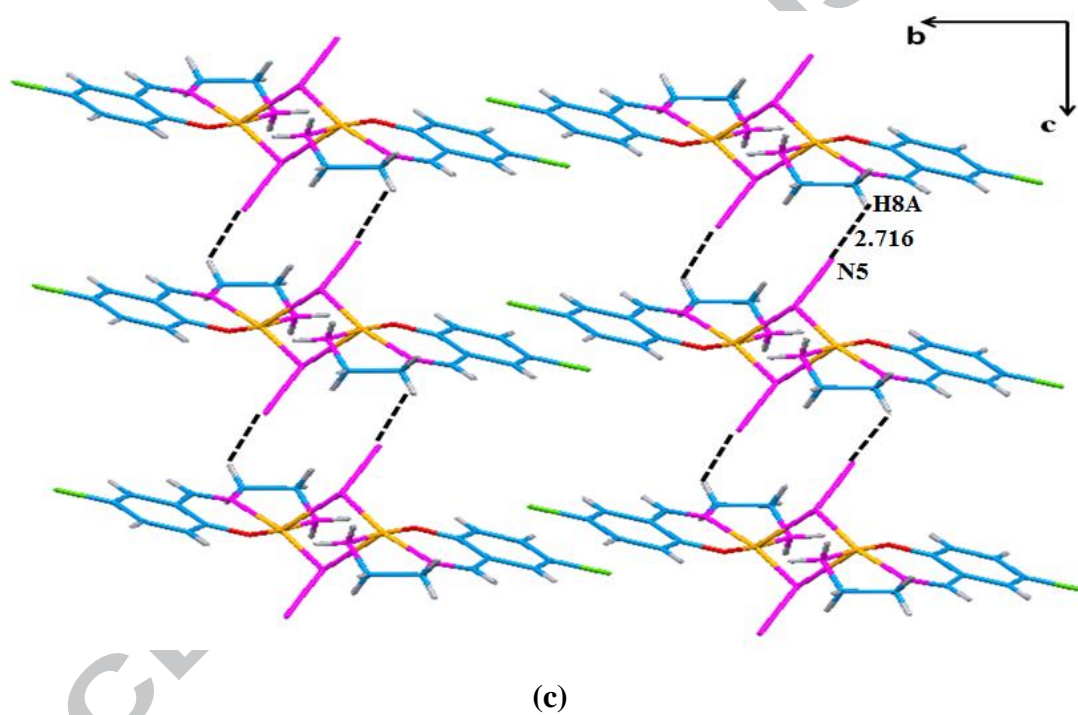
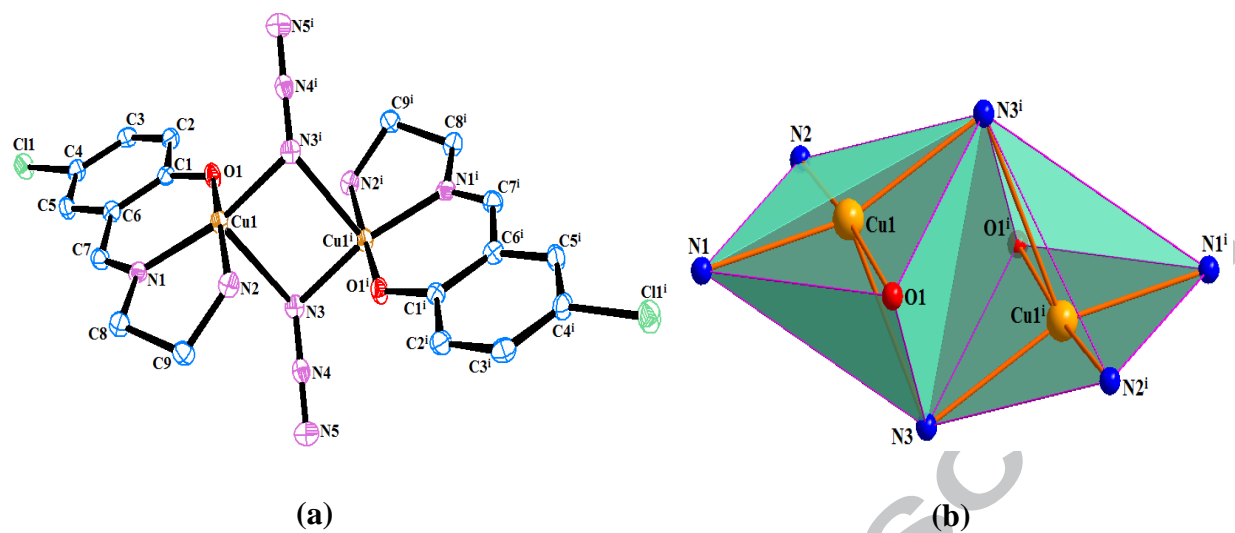
**Table 2.** Selected bond lengths ( $\text{\AA}$ ) and angles ( $^\circ$ ) for **1** and **2**.

<b>1</b>			
Bond lengths ( $\text{\AA}$ )			
Cu(1)-Cu(1)#1	3.1593(11)	Cu(1)-N(3)	2.001(2)
Cu(1)-O(1)	1.920(2)	Cu(1)-N(2)	2.005(2)
Cu(1)-N(1)	1.949(2)	Cu(1)-N(3)#1	2.470(2)
Bond angles ( $^\circ$ )			
Cu(1)-N(3)-Cu(1)#1	89.30(8)	N(1)-Cu(1)-N(2)	84.81(8)
O(1)-Cu(1)-N(1)	93.39(8)	O(1)-Cu(1)-N(2)	174.28(8)
N(1)-Cu(1)-N(3)	164.08(8)	O(1)-Cu(1)-N(3)	90.86(7)
<b>2</b>			
Bond lengths ( $\text{\AA}$ )			
Co-O(1)	1.8930(16)	Co-N(4)	1.9068(19)
Co-O(2)	1.8932(16)	Co-N(2)	1.950(2)
Co-N(1)	1.9004(19)	Co-N(3)	1.954(2)
Bond angles ( $^\circ$ )			
O(1)-Co-O(2)	91.30(7)	O(2)-Co-N(4)	94.23(8)
O(1)-Co-N(1)	94.93(8)	N(1)-Co-N(4)	177.40(8)
O(2)-Co-N(1)	87.51(7)	O(1)-Co-N(2)	179.25(8)
O(1)-Co-N(4)	86.97(7)	HW(1A)-OW(1)-HW(1B)	103(2)

Symmetry transformations used to generate equivalent atoms: #1 -x,-y+2,-z+1 for **1**.

### 3.2 . Crystal structure description

**3.2.1. Structure of  $[\text{Cu}(\text{L})(\text{N}_3)]_2(\mathbf{1})$ :**  $\mathbf{1}$  crystallizes in the triclinic space group  $P\bar{1}$ . The Cu(II) ion is in a square pyramidal arrangement with the ligand nitrogen atoms (N1 and N2), phenoxo oxygen atom (O1) and azide nitrogen atom (N3) occupying the base of the pyramid, and the symmetry related azido N atom (N3') occupying the apex of the pyramid (Figures 1a and b). The Cu atom deviates by  $\sim 0.1 \text{ \AA}$  from the square plane. The azide ligand acts as an asymmetric  $\mu$ -1,1 bridge and connects the Cu1 atom to its inversion related unit. The Cu centers within the dimer are separated by  $3.1593(11) \text{ \AA}$ . The crystal packing (Figures 1c and 1d) is stabilized by intramolecular C-H $\cdots$ N ( $2.716 \text{ \AA}$ ), N-H $\cdots$ O ( $\text{H}\cdots\text{N} = 2.583 \text{ \AA}$ ) and C-H $\cdots$ Cl ( $\text{H}\cdots\text{Cl} = 2.885 \text{ \AA}$ ) hydrogen bonding interactions (Table 3). Although there are plenty of asymmetrically end-on azide bridged Cu(II) dimers in the reported literature, asymmetric basal-apical end-on azide bridged Cu(II) dimers with half condensed Schiff base ligands are rather limited. Among the reported dimers, the ones structurally quite close to  $\mathbf{1}$  are  $[\text{Cu}_2\text{L}_2(\text{N}_3)_2]$  ( $\text{L} = 1\text{-(N-salicylideneamino)-2-aminoethane}$ )<sup>[5a]</sup>,  $[\text{CuL}(\mu\text{-}1,1\text{-N}_3)]_n$  ( $\text{L} = 4\text{-chloro-2-[(2-dimethylaminoethylimino)methyl]phenolate}$ )<sup>[27]</sup>,  $[\text{Cu}_2\text{L}_2(\mu\text{-}1,1\text{-N}_3)_2]\cdot\text{H}_2\text{O}\cdot\text{CH}_3\text{OH}$  ( $\text{L} = 1\text{-(N-ortho-hydroxyacetophenimine)-2-aminoethane}$ )<sup>[25b]</sup>,  $[\text{Cu}(\text{L}^2)_2(\mu\text{-}1,1\text{-N}_3)_2]$  ( $\text{L}^2 = \text{N}_2\text{O}$  half condensed Schiff base of naphthaldehyde and N,N-dimethyl diaminopropane) and  $[\text{Cu}(\text{L}^4)_2(\mu\text{-}1,1\text{-N}_3)_2]$  ( $\text{L}^4 = \text{N}_2\text{O}$  half condensed Schiff base of naphthaldehyde and N,N-diethyl diaminopropane).<sup>[20]</sup> The coordination behavior of the ligand, Cu-N distances and angles at the azide bridge in  $\mathbf{1}$  are similar to these reported systems. Structural parameters relevant for magnetic discussion are tabulated in Table 4.



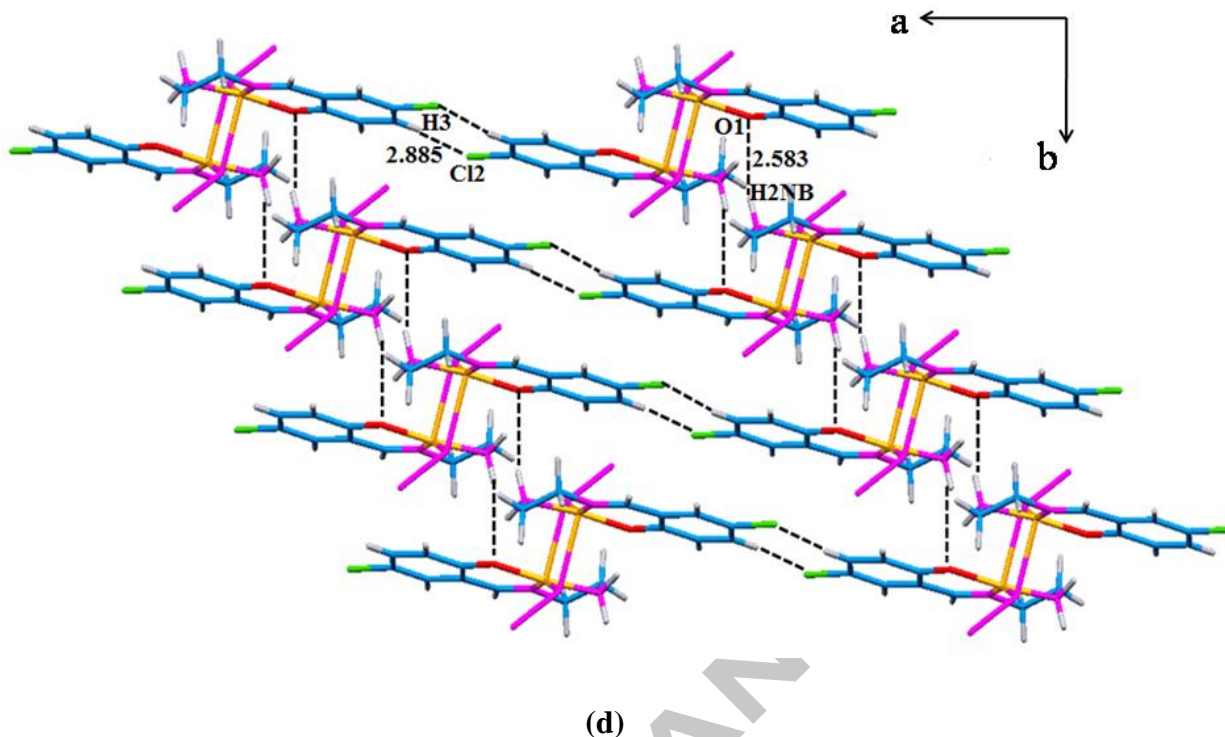
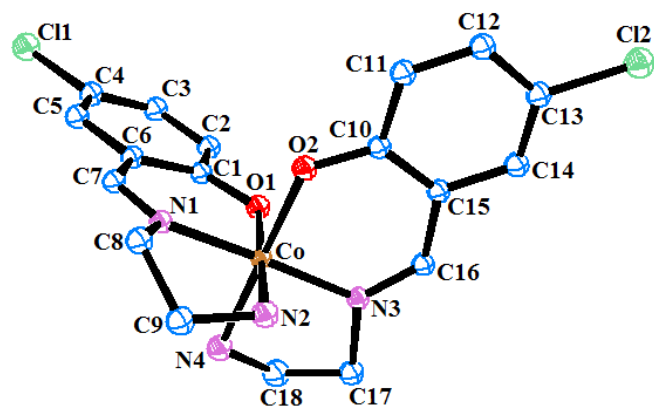


**Figure 1 (a).** ORTEP of **1** showing atoms as 40% probability ellipsoids. Symmetry code:  $i = -x, -y+2, -z+1$ , **(b)** Polyhedra of Cu1 and Cu1<sup>i</sup> atoms showing a distorted square pyramidal geometry, **(c-d)** Crystal packing of **1** showing hydrogen bond interactions which form the supramolecular network.

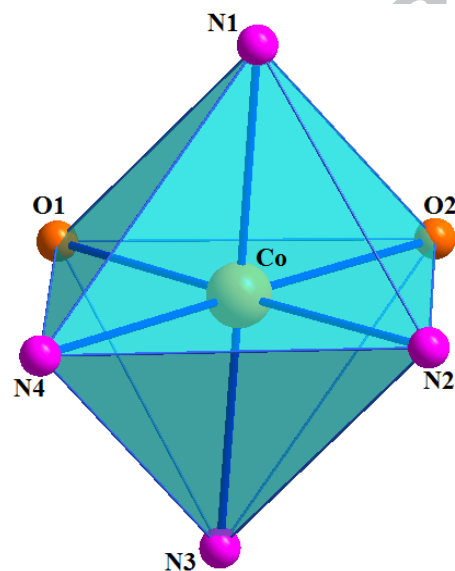
### 3.2.2. Structure of [Co(L)<sub>2</sub>]<sub>3</sub>·H<sub>2</sub>O (**2**):

Complex **2** crystallizes in the monoclinic space group  $P2_1/c$ . The Co(III) ion is octahedrally coordinated by two imine nitrogen atoms, two phenolic oxygen atoms and two amine nitrogen atoms of the two Schiff base ligands (Figures 2a and 2b). The phenoxo oxygen atoms (O1 and O2) and amine nitrogen atoms (N2 and N4) form the base of the square plane and the imino nitrogen atoms (N1 and N3) occupy the axial positions of the octahedron. The crystal packing is shown in Figure 2c. There is one uncoordinated azide anion in the unit cell which hydrogen bonds with solvent water hydrogen atoms to form and stabilize the supramolecular network. The packing structure is further stabilized by C-H $\cdots$ Cl interactions ( $H\cdots Cl = 2.89-2.93$  Å), O-H $\cdots$ N ( $H\cdots N = 2.089-2.81$  Å) and N-H $\cdots$ N ( $H\cdots N = 1.929-2.201$  Å) interactions, propagating a 2-D network of 1-D chains formed by C-H $\cdots$ Cl interactions (Table 3). Such weak C-H $\cdots$ Cl

interactions, in the range 2.84-2.92 Å for H $\cdots$ Cl, have been previously reported in Co(III) systems<sup>[28]</sup> and in a (4-benzylpyridinium) tetrachloro cuprate(II) complex in the range 2.42-2.78 Å.<sup>[29]</sup>



(a)



(b)

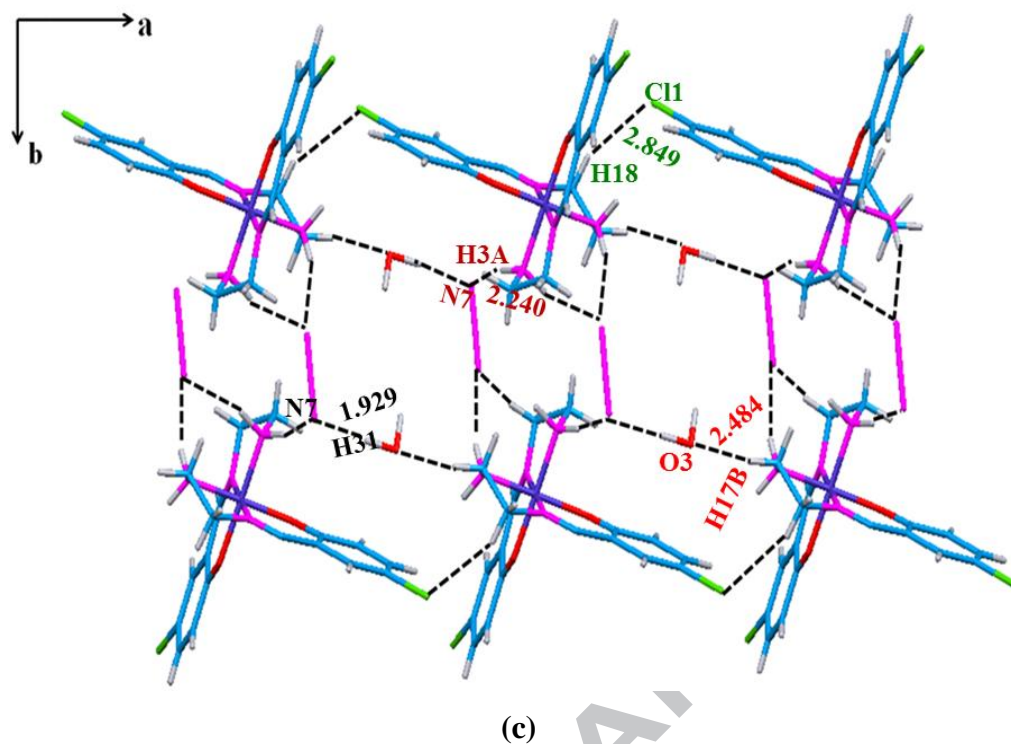


**Figure 2 (a).** ORTEP of **2** showing atoms as 40% probability ellipsoids; solvent water and uncoordinated azide molecules have been omitted for clarity **(b)** Polyhedron of the Co(III) ion showing a distorted octahedral geometry; **(c)** Crystal packing of **2** showing hydrogen bonding interactions propagating the supramolecular network.

Table 3. Hydrogen-bonding distances (Å) and angles (°) for complexes **1** and **2**.

Compound	D-H...A	D-H	H...A	D...A	<D-H...A
<b>1</b>	N(2)-H(2NB)...O(1)#2	0.89	2.58	3.449(3)	164.5
	N(2)-H(2NB)...N(3)#3	0.89	2.57	3.107(3)	119.6
	C(3)-H(3)...Cl(2)#4	0.93	2.88	3.761(3)	157.5
	C(7)-H(8)...Cl(2)#5	0.93	2.99	3.612(3)	125.8
	C(9)-H(9B)...N(4)#1	0.97	2.70	3.400(3)	129.4
<b>2</b>	C(3)-H(3)...OW1#1	0.93	2.55	3.291(3)	137.3
	C(7)-H(7)...O(1)#2	0.93	2.43	3.172(3)	137.1
	C(8)-H(8A)...N(5)	0.97	2.64	3.391(4)	134.6
	C(9)-H(9B)...Cl(2)#3	0.97	2.93	3.715(3)	138.8
	C(10)-H(10A)...OW1#4	0.97	2.54	3.159(3)	121.3
	C(11)-H(11B)...Cl(2)#5	0.97	2.89	3.765(3)	150.3
	C(12)-H(12)...N(7)#6	0.93	2.46	3.348(3)	161.0
	OW1-HW1A...N(6)	0.862(10)	2.81(2)	3.529(3)	142(3)
	OW1-HW1A...N(7)	0.862(10)	2.089(15)	2.926(3)	164(3)
	OW1-HW1B...Cl(1)#7	0.861(10)	2.93(3)	3.513(2)	126(3)
	OW1-HW1B...Cl(1)#2	0.861(10)	2.81(4)	3.367(2)	124(3)

Symmetry transformations used to generate equivalent atoms:

#1 -x, -y+2, -z+1; #2 x+1, y, z; #3 -x+1, -y+2, -z+1; #4 -x-2, -y+2, -z+2; #5 -x-1, -y+1, -z+2 for **1** and #1 -x, y+1/2, -z+1/2; #2 x, -y+3/2, z+1/2; #3 x, y, z+1; #4 -x, -y+1, -z+1; #5 x-1, y, z; #6 x, y, z-1; #7 -x, y-1/2, -z+1/2 for **2**.

#### 4. Hirshfeld surface analysis

The Hirshfeld surfaces for both complexes **1** and **2**, mapped over  $d_{\text{norm}}$ , are shown in Figures 3a and 3b. Each molecule in the asymmetric unit of a given crystal structure has a unique Hirshfeld surface. Transparent surfaces allow visualization of the molecular moiety around which they are calculated. The red spots on the  $d_{\text{norm}}$  surface indicate hydrogen bond contacts, as well as other weak interactions. Hirshfeld surface analysis provides a visual way to evaluate the percentage contribution of the various intermolecular interactions in the crystal packing. It has great influence to explore the packing adaptation of a crystal in a unit cell through various types of intermolecular interactions. Thus, we employed Hirshfeld surface analysis to study such interactions present in the structure and provide a powerful tool to explain the adaption of different crystal-packing structures.<sup>[18, 30]</sup>

The percentage contributions of various types of intermolecular interactions in the fingerprint, such as  $\text{H}\cdots\text{H}$ ,  $\text{C}\cdots\text{H}$ ,  $\text{Cl}\cdots\text{H}$ ,  $\text{N}\cdots\text{H}$ ,  $\text{N}\cdots\text{C}$ ,  $\text{O}\cdots\text{H}$  and  $\text{C}\cdots\text{C}$ , are shown as a bar graph in Figure 3c. The 2D fingerprint plot presented in Figure S2., provides a summary of each combination of  $d_e$  and  $d_i$  across the surface of the molecule.

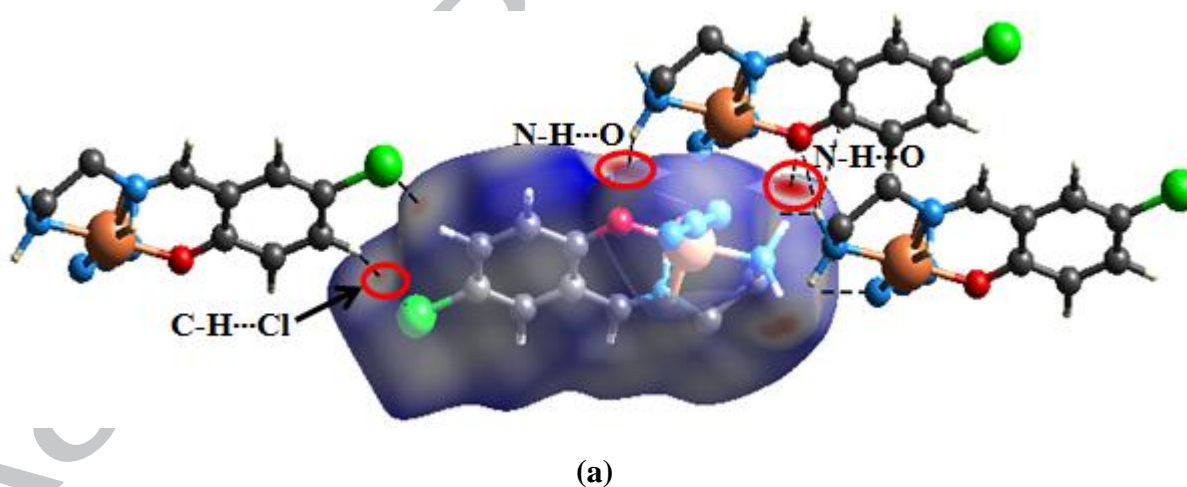
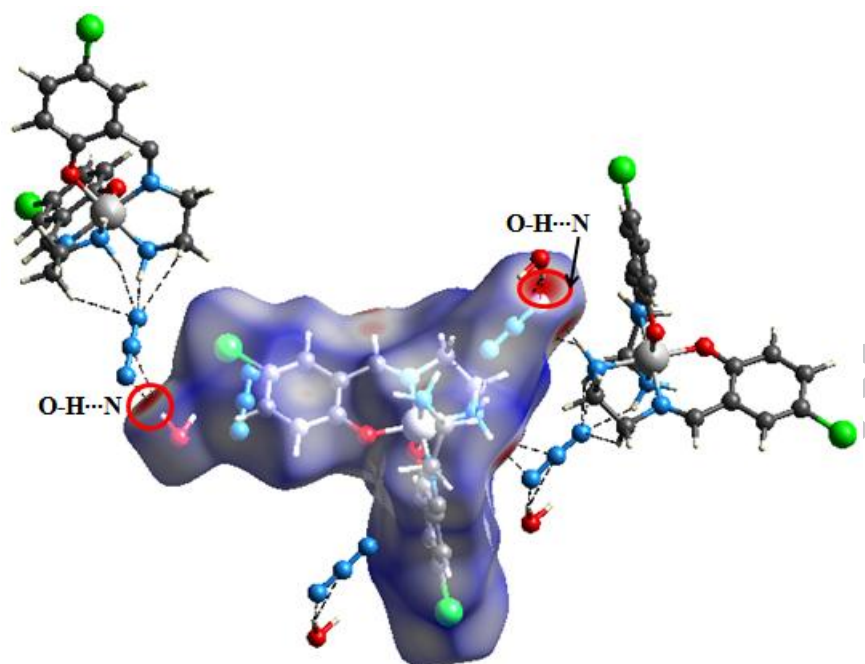
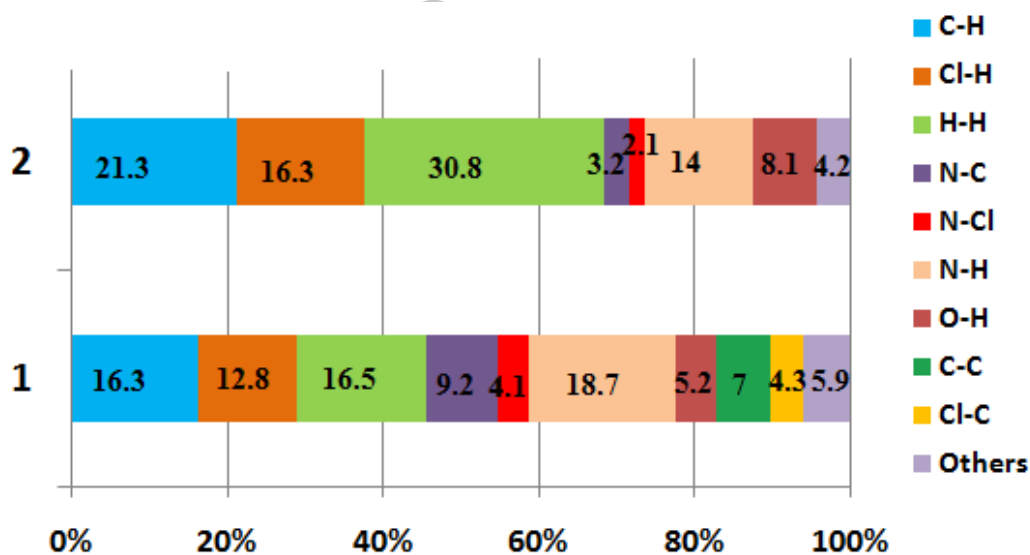


**Figure 3a.** Hirshfeld surface of complex **1** mapped with  $d_{\text{norm}}$  showing short range  $\text{N-H}\cdots\text{O}$  and  $\text{C-H}\cdots\text{Cl}$  interactions.



(b)

**Figure 3b.** Hirshfeld surface of complex **2** mapped with  $d_{\text{norm}}$  showing short range O-H...N interactions.

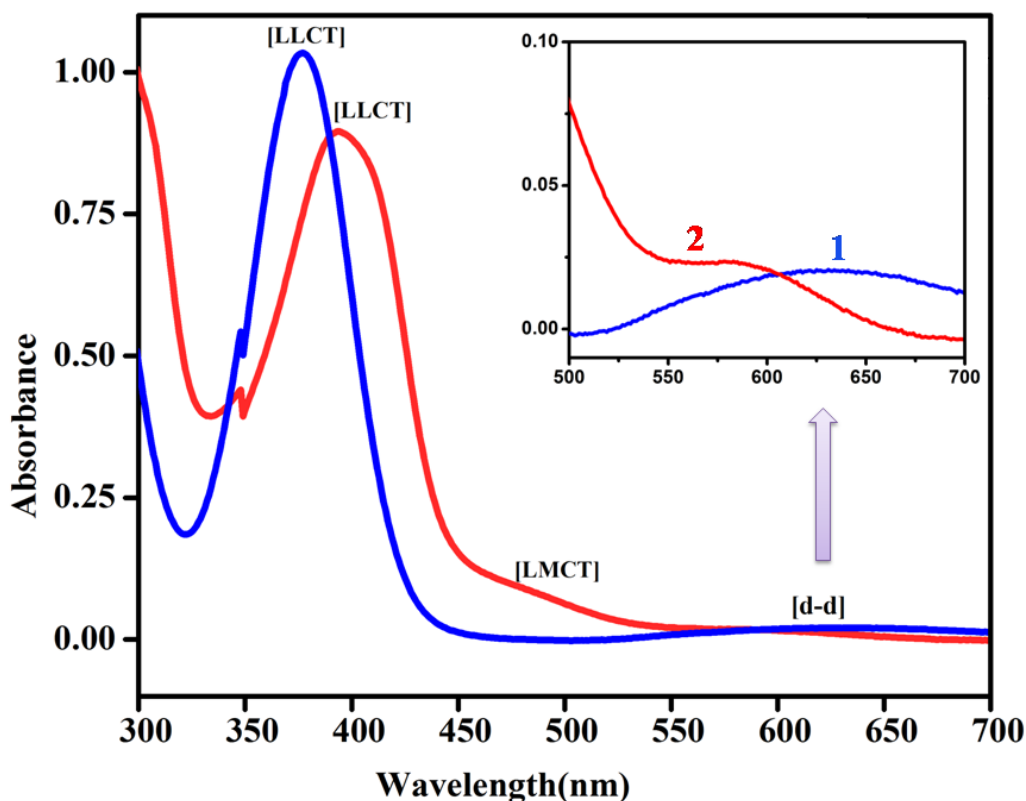


(c)

**Figure 3c.** Relative contributions of the various intermolecular contacts to the Hirshfeld surface areas in complex **1** and **2**.

## 5. Electronic spectra

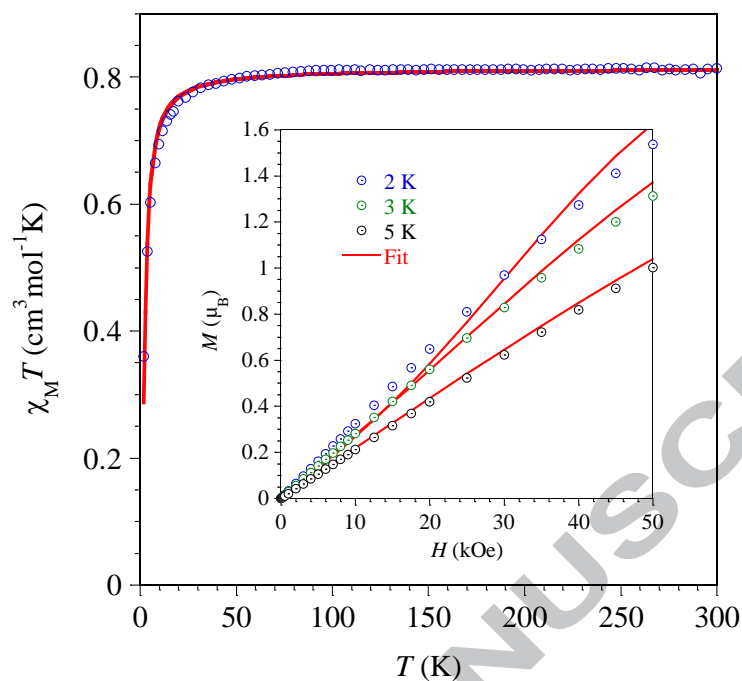
The solution state absorption spectra for both complexes were recorded in DMSO and are presented in Figure 4. Complex **1** shows two bands, a band centered between 365 and 420 nm ( $\lambda_{\text{max}}$  at 377 nm) due to a ligand to ligand charge transfer (LLCT), while a broad band between 530 and 690 nm ( $\lambda_{\text{max}}$  at 617 nm) is assigned to d-d transitions of the metal ion. For complex **2**, three bands were observed. A band centered between 360 and 490 nm ( $\lambda_{\text{max}}$  at 393 nm) is assigned to a ligand-ligand charge transfer (LLCT), while a band centered between 460 and 530 nm ( $\lambda_{\text{max}}$  at 487 nm) is due to a ligand to metal charge transfer (LMCT). The third broad band between 550 and 680 nm ( $\lambda_{\text{max}}$  at 595 nm) is assigned to d-d transitions of the metal ion.<sup>[31]</sup>



**Figure 4.** UV-visible spectra of complexes **1** and **2** in DMSO solvent. (Inset) Enlarged view of the d-d transition band.

## 6. Magnetic properties

The temperature dependence for  $\chi_M T$  ( $\chi_M$  stands for the molar magnetic susceptibility calculated for the  $\text{Cu}_2$  unit) found for **1** (Figure 5) is characteristic for a weak antiferromagnetic interaction, in agreement with the axial-equatorial  $\text{N}_3$ -linkage between the two centers.<sup>[32]</sup> At 300 K, a value of  $0.81 \text{ cm}^3 \text{ mol}^{-1} \text{ K}$  was found for  $\chi_M T$ , in agreement with the contribution of two non-interacting  $\text{Cu(II)}$  centers. This value remains unchanged as  $T$  is lowered to ca 50 K, below which temperature it rapidly decreases to reach  $0.36 \text{ cm}^3 \text{ mol}^{-1} \text{ K}$  at 2 K. A Curie-Weiss analysis of  $\chi_M^{-1} = f(T)$  for the susceptibility data per Cu atom above 20 K (Fig. S4) led to  $C = 0.40 \text{ cm}^3 \text{ mol}^{-1}$  and  $\theta = -0.83 \text{ K}$ . The isothermal field dependence of the magnetization (Figure. 5 inset) recorded at 2, 3 and 5 K is in agreement with a rather weak antiferromagnetic interaction between the Cu centers. The strength of the Cu-Cu exchange interaction was assessed by analyzing the  $\chi_M T$  behavior using the Bleaney-Bowers expression for a  $S = 1/2$  dimer (derived from the phenomenological Hamiltonian  $H = -J\mathbf{S}_A \cdot \mathbf{S}_B$ ).<sup>[33]</sup> The best fit to the experimental behavior yielded an exchange parameter of  $J = -2.93 \pm 0.03 \text{ cm}^{-1}$  and  $g = 2.084 \pm 0.001$  (Fig. S5). The same result was obtained when the analysis was performed simultaneously on  $\chi_M T$  and the magnetization behaviors using PHI,<sup>[34]</sup> yielding  $J = -2.93 \pm 0.05 \text{ cm}^{-1}$  and  $g = 2.083 \pm 0.003$ . The calculated behaviors well fit to the experimental data (Figure. 5), except for a slight discrepancy for magnetization at 2 K. This was not improved when possible intermolecular interactions were taken into account. These results confirm that the exchange interactions mediated by the 1,1- $\text{N}_3$  bridges in **1** are weak.

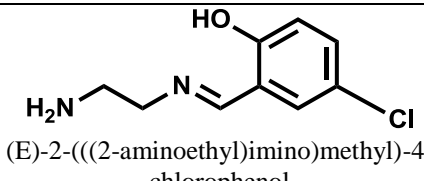
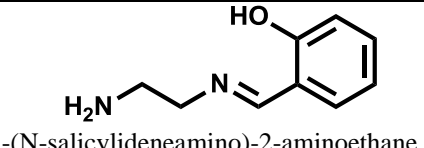
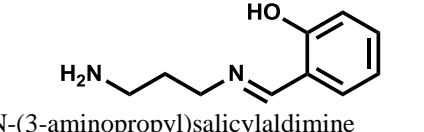
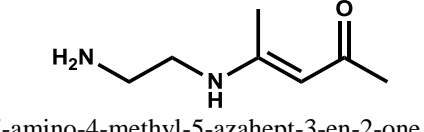
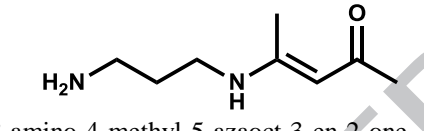
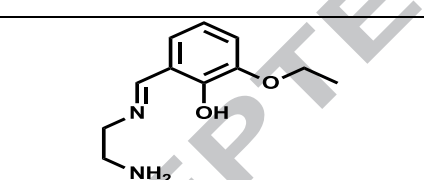


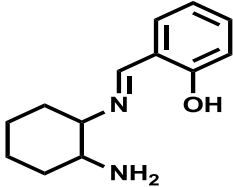
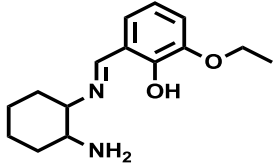
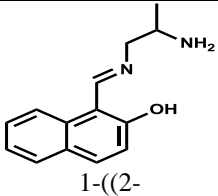
**Figure 5:** Experimental (○) and calculated (—) temperature dependence of  $\chi_M T$  and (inset) field-dependence of the magnetization for different temperatures between 2 and 5 K; best fit parameters are discussed in the main text.

Magneto-structural parameters for double  $\mu_{1,1}$ -azide bridged half condensed Schiff base dimers are summarized in Table 4. The observed magnetic behaviour of **1** is in accordance with the behaviour of reported systems.

Complex **2** was found to be diamagnetic, in agreement with the low spin configuration for a Co(III) ion in such an octahedral coordination sphere.

**Table 4.** Structural and magnetic parameters of reported double  $\mu_{1,1}$ -N<sub>3</sub> bridged half condensed Schiff base copper(II) complexes.

S. No.	Compound	Ligand	Cu-Cu Å	Cu-N <sub>azido</sub> (basal) Å	Cu-N <sub>azido</sub> (apical) Å	Cu-N-Cu (°)	J <sub>1</sub> cm <sup>-1</sup>	Geometry around Cu(II)
1	[CuL( $\mu_{1,1}$ -N <sub>3</sub> )] <sub>2</sub> <sup>*</sup>	 (E)-2-(((2-aminoethyl)imino)methyl)-4-chlorophenol	3.1593(11)	1.949(2) and 2.005(2)	2.001(2) and 2.470(2)	89.30(8)	-2.93(3)	dist. Sq. Py
2	[Cu <sub>2</sub> (L1) <sub>2</sub> (N <sub>3</sub> ) <sub>2</sub> ] <sup>5a</sup>	 1-(N-salicylideneamino)-2-aminoethane	3.1807(9)	1.998	2.505(3)	89.1	-8.5(5)	dist. Sq. Py
3	[Cu <sub>2</sub> (L2) <sub>2</sub> (N <sub>3</sub> ) <sub>2</sub> ] <sup>5b</sup>	 N-(3-aminopropyl)salicylaldimine	3.193	2.039(7)	2.440(7)	90.50	-1.8	tri. dist. Sq. Py
4	[Cu <sub>2</sub> (L3) <sub>2</sub> (N <sub>3</sub> ) <sub>2</sub> ] <sup>5b</sup>	 7-amino-4-methyl-5-azahept-3-en-2-one	3.161	2.020(4)	2.546(5)	86.82	-3.1	tri. dist. Sq. Py
5	[Cu <sub>2</sub> (L4) <sub>2</sub> (N <sub>3</sub> ) <sub>2</sub> ] <sup>5b</sup>	 8-amino-4-methyl-5-azaoct-3-en-2-one	3.318	2.060(8)	2.475(9)	93.60	+2.9	tri. dist. Sq. Py
6	[Cu(L5)( $\mu_{1,1}$ -N <sub>3</sub> )] <sub>2</sub> <sup>13b</sup>	 (E)-2-(((2-aminoethyl)imino)methyl)-6-ethoxyphenol	3.1208(5)	1.984(18)	2.489(19)	87.71(7)	-10.16	dist. Sq. Py

7	$[\text{Cu}(\text{L6})(\mu_{1,1}\text{-N}_3)_2]^{13\text{b}}$	 <p>(E)-2-((2-aminocyclohexyl)imino)methylphenol</p>	3.227(2)	2.005(5)	2.5005(5)	90.83(18)	-4.18	dist. Sq. Py
8	$[\text{Cu}(\text{L7})(\mu_{1,1}\text{-N}_3)_2]^{13\text{b}}$	 <p>(E)-2-((2-aminocyclohexyl)imino)methyl-6-ethoxyphenol</p>	3.070(17)	1.983(5)	2.551(6)	84.3(2)	-1.43	dist. Sq. Py
9	$[\text{Cu}_2(\text{L8})_2(\text{N}_3)_2] \cdot \text{DMF}^{35}$	 <p>1-((2-aminopropyl)imino)methylnaphthalen-2-ol</p>	3.1785(8), 3.1822(7)	1.984(4), 1.995(3)	2.646(4), 2.577(4)	85.4(1), 87.2(1)	+9.6	dist. Sq. Py

Note: Superscript indicates the reference number.

\*Present complex 1, dist. Sq. py = distorted square pyramid, tri. dist. Sq. py = trigonally distorted square pyramid.

## 7. Conclusions

The nature of the Schiff base formed (fully or half condensed) with its differing ligating characteristics (tetra- or tridentate) can modify the coordination geometry of a metal ion and in association with auxiliary ligands, like azide or thiocyanate, may have important implications on the magnetic behaviour. Previously we have demonstrated the formation of tetranuclear clusters of Cu(II) ions involving salpn/salophen as the Schiff base and azide as an auxiliary ligand.<sup>[18]</sup> To observe the role of a chloro substituent on the aldehyde of the Schiff base, on the structural changes and associated magnetic properties, our attempts have resulted in the isolation of the title complexes, templated by the metal ion, in which the Schiff base is only half condensed, irrespective of the amine to aldehyde molar ratios. Complex **1** is an asymmetric  $\mu_{-1,1}$  azide bridged dimer displaying weak antiferromagnetic interactions ( $J = -2.93 \text{ cm}^{-1}$ ), in agreement with the axial-equatorial  $\text{N}_3^-$ -linkage between the two copper centres. Complex **2** is a monomer of low spin Co(III) ions, as evidenced by structure and cyclic voltammetry studies. These examples provide a direction towards the deliberate synthesis of half condensed Schiff base complexes and further investigations on the preparation of half condensed Schiff base complexes by modifying the aldehyde and amine environments as well as the nature of the metal ions in templating the SB formation are in progress.

## Appendix A. Supplementary data

Supplementary data includes IR spectra of complexes **1** and **2** in Figure S1. The 2D fingerprint plot of the Hirshfeld analysis is presented as Figure S2. The cyclic voltammogram of complex **2** is shown as Figure S3. CCDC Nos. 1875686 and 1875687 contains supplementary crystallographic data for complexes **1** and **2** respectively. These data can be obtained free of charge via <http://www.ccdc.cam.ac.uk/conts/retrieving.html>, or from the Cambridge Crystallographic Data Centre, 12 Union Road, Cambridge CB2 1EZ, UK; fax: (+44) 1123-336-033; or e-mail: [deposit@ccdc.cam.ac.uk](mailto:deposit@ccdc.cam.ac.uk).

**Conflicts of interest:**

There are no conflicts of interest to declare.

**Acknowledgements**

Financial assistance from DST, New Delhi, India for the project YSS/2015/000993 is gratefully acknowledged. Prof. Hiroshi Nishihara's laboratory at The University of Tokyo, Tokyo, Japan for the X-ray data of **1** and the Department of Chemistry, IIT Kanpur, India is gratefully acknowledged for the X-ray data of **2**. SSS thanks the JSPS, Japan for the bridge fellowship for the visit to Prof. Hiroshi Nishihara's laboratory at The University of Tokyo, Tokyo, Japan.

**Keywords:** Half condensed Schiff base complexes, Cu(II) and Co(III) ions, azide, structure, magnetic properties

**References:**

- [1].(a) J. Schmid, W. Frey, R. Peters, *Organometallics*, 36 (2017) 4313–4324; (b) X. Zhang, Y. Zhu, X. Zheng, D. Phillips, C. Zhao, *Inorg. Chem.*, 53 (2014) 3354–3361; (c) A. Bhattacharjee, S. Halder, K. Ghosh, C. Rizzoli, P. Roy, *New J. Chem.*, 41 (2017) 5696–5706; (d) I. Bratko, M. Gómez, *Dalton Trans.*, 42 (2013) 10664–10681.
- [2]. (a) Z. Gu, J. Na, B. Wang, H. Xiao, Z. Li, *CrystEngComm.*, 13 (2011) 6415–6421; (b) Z. Meng, L. Yun, W. Zhang, C. Hong, R. Herchel, Y. Ou, J. Leng, M. Peng, Z. Lin, M. Tong, *Dalton Trans.*, 0 (2009) 10284–10295; (c) H. Zhang, C. Xue, J. Shi, H. Liu, Y. Dong, Z. Zhao, D. Zhang, J. Jiang, *Cryst. Growth Des.*, 16 (2016) 5753–5761; (d) A. Escuer, J. Esteban, S. Perlepes, T. Stamatatos, *Coord. Chem. Rev.*, 275 (2014) 87–129; (e) C. Maxim, F. Tuna, A. Madalan, N. Avarvari, M. Andruh, *Cryst. Growth Des.*, 12 (2012) 1654–1665.
- [3].(a) Y. Han, N. Chilton, M. Li, C. Huang, H. Xu, H. Hou, B. Moubaraki, S. Langley, S. Batten, Y. Fan, K. Murray, *Chem. Eur. J.*, 19 (2013) 6321–6328; (b) A. Casini, B. Woods, M. Wenzel, *Inorg. Chem.*, 56 (2017) 14715–14729; (c) L. Huo, L. Gao, J. Gao, F. An, X. Niu, T. Hu, *Inorg. Chem. Commun.*, 89 (2018) 83–88; (d) M. Zhang, T. Fan, Q. Wang, H. Han, X. Li,

- J. Solid State Chem.*, 258 (2018) 744–752; (e) F. Yuan, C. Yuan, H. Hu, T. Wang, C. Zhou, *J. Solid State Chem.*, 258 (2018) 588–601.
- [4]. (a) M. Chen, M. Chen, C. Zhou, W. Lin, J. Chen, W. Chen, Z. Jiang, *Inorg. Chim. Acta.*, 405 (2013) 461–469; (b) J. Chen, W. Lin, C. Zhou, L. Yau, J. Wang, B. Wang, W. Chen, Z. Jiang, *Inorg. Chim. Acta.*, 376 (2011) 389–395.
- [5]. (a) S. Koner, S. Saha, T. Mallah, K. Okamoto, *Inorg. Chem.*, 43 (2004) 840–842; (b) M. Ray, A. Ghosh, R. Bhattacharya, G. Mukhopadhyay, M. Drew, J. Ribas, *Dalton Trans.* (2004) 252–259.
- [6]. (a) M. Sarkar, R. Clérac, C. Mathonière, N. Hearn, V. Bertolasi, D. Ray, *Inorg. Chem.*, 50 (2011) 3922–3933; (b) S. Biswas, S. Naiya, C. Gómez-García, A. Ghosh, *Dalton Trans.*, 41 (2012) 462–473.
- [7]. (a) Y. Zeng, J. Zhao, B. Hu, X. Hu, F. Liu, J. Ribas, J. Ribas-Ariño, X. Bu, *Chem. Eur. J.*, 13 (2007) 9924–9930; (b) A. Bartyzel, *Polyhedron*, 134 (2017) 30–40; (c) Song, K. Lim, D. Ryu, S. Yoon, B. Suh, C. Hong, *Inorg. Chem.*, 53 (2014) 7936–7940.
- [8]. (a) P. Mukherjee, M. Drew, A. Ghosh, *Eur. J. Inorg. Chem.*, (2008) 3372–3381; (b) A. D. Khalaji, S. Triki, *Russ J. Coord. Chem.*, 38 (2012) 579–582; (c) A. Khalaji, H. Stoekli-Evans, *Polyhedron*, 28 (2009) 3769–3773.
- [9]. (a) M. Ray, A. Ghosh, S. Chaudhuri, M. Drew, J. Ribas, *Eur. J. Inorg. Chem.*, (2004) 3110–3117; (b) R. Hui, P. Zhou, Z. You, *Russ. J. Coord. Chem.*, 36 (2010) 525–529; (c) J. Zhang, X. Zhou, X. Wang, X. Li, Z. You, *Transition Met. Chem.*, 36 (2011) 93–98.
- [10]. S. Jana, B. Shaw, P. Bhowmik, K. Harms, M. Drew, S. Chattopadhyay, S. Saha, *Inorg. Chem.*, 53 (2014) 8723–8734.
- [11]. (a) N. Zare, A. Zabardasti, M. Dusek, V. Eigner, *J. Mol. Struct.*, 1163 (2018) 388–396; (b) M. Kalhor, Z. Seyedzade, *Res. Chem. Intermed.*, 43 (2017) 3349–3360.
- [12]. (a) J. Costes, C. Duhayan, L. Vendier, *Polyhedron*, 153 (2018) 158–162; (b) V. Béreau, S. Dhers, J. P. Costes, C. Duhayan, J. P. Sutter, *Eur. J. Inorg. Chem.* (2018) 66–73.

- [13]. (a) P. Bhowmik, S. Jana, S. Chattopadhyay, *Polyhedron*, 44 (2012) 11–17; (b) S. Mondal, P. Chakraborty, N. Aliaga-Alcalde, S. Mohanta, *Polyhedron*, 63 (2013) 96–102.
- [14]. (a) R. C. Elder, *Aust. J. Chem.*, 31 (1978) 35–45; (b) S. Naiya, H. Wang, M. Drew, Y. Song, A. Ghosh, *Dalton Trans.*, 40 (2011) 2744–2756.
- [15]. (a) S. Koner, S. Saha, K. Okamoto, J. Tuchagues, *Inorg. Chem.*, 42 (2003) 4668–4672; (b) I. Pankov, I. Shcherbakov, V. Tkachev, S. Levchenkov, L. Popov, V. Lukov, S. Aldoshin, V. Kogan, *Polyhedron*, 135 (2017) 237–246.
- [16]. (a) S. Mukherjee, P. Mukherjee, *Cryst. Growth Des.* 14 (2014) 4177–4186; (b) S. Naiya, C. Biswas, M. Drew, C. Gómez-García, J. Clemente-Juan, A. Ghosh, *Inorg. Chem.*, 49 (2010) 6616–6627; (c) S. Majumder, S. Sarkar, S. Sasmal, E. Sañudo, S. Mohanta, *Inorg. Chem.*, 50 (2011) 7540–7554.
- [17]. (a) P. Seth, S. Ghosh, A. Figuerola, A. Ghosh, *Dalton Trans.*, 43 (2014) 990–998; (b) B. K. Babu, A. R. Biju, S. Sunkari, M. V. Rajasekharan, J. Tuchagues, *Eur. J. Inorg. Chem.*, (2013) 1444–1450.
- [18]. P. Pandey, N. Dwivedi, G. Cosquer, M. Yamashita, S. Sunkari, *ChemistrySelect*, 3 (2018) 10311–10319.
- [19]. S. Sahadevan, E. Cadoni, N. Monni, C. Pipaón, J. Mascaros, A. Abhervé, N. Avarvari, L. Marchiò, M. Arca, M. Mercuri, *Cryst. Growth Des.*, 18 (2018) 4187–4199.
- [20]. S. Jana, B. Shaw, P. Bhowmik, K. Harms, M. Drew, S. Chattopadhyay, S. Saha, *Inorg. Chem.*, 53 (2014) 8723–8734.
- [21]. G. M. Sheldrick, *Acta Cryst. A.*, 64 (2008) 112–122.
- [22]. M. N. Burnett, C. K. Johnson, Report ORNL–6895. Oak Ridge National Laboratory, Oak Ridge, Tennessee, (1996).
- [23]. I. J. Bruno, J. C. Cole, P. R. Edgington, M. K. Kessler, C. F. Macrae, P. McCabe, J. Pearson, R. Taylor, *Acta Cryst. B.*, 58 (2002) 389–397.
- [24]. S. K. Wolff, D. J. Grimwood, J. J. McKinnon, D. Jayatilaka, M. A. Spackman, *Crystal*

- Explorer 2.1, University of Western Australia, Perth, Australia, (2007).
- [25]. (a) M. S. Ray, A. Ghosh, S. Chaudhuri, M. G. B. Drew, J. Ribas, *Eur. J. Inorg. Chem.*, (2004) 3110–3117; (b) M. Zbiri, S. Saha, C. Adhikary, S. Chaudhuri, C. Daul, S. Koner, *Inorg. Chim. Acta.*, 359 (2006) 1193–1199.
- [26]. (a) P. Pandey, B. Kharediya, B. Elrez, J.-P. Sutter, S. Sunkari, *J. Coord. Chem.*, 70 (2017) 1237–1246; (b) P. Pandey, B. Kharediya, B. Elrez, J.-P. Sutter, G. Bhargavi, M. V. Rajasekharan, S. Sunkari, *Dalton Trans.*, 46 (2017) 15908–15918.
- [27] Z. You, Q. Jiao, S. Niu, J. Chi, *Z. Anorg. Allg. Chem.*, 632 (2006) 2481–2485.
- [28] N. Salem, A. Rashad, L. El Sayed, W. Haase, M. Iskander, *Polyhedron*, 68 (2014) 164–171.
- [29] K. Azouzi, B. Hamdi, R. Zouari, A. Ben Salah, *Ionics*, 22 (2016) 1669–1680.
- [30] (a) N. Dwivedi, S. Panja, Monika, S. Saha, S. Sunkari, *Dalton Trans.*, 45 (2016) 12053–12068; (b) M. Masoudi, M. Behzad, A. Arab, A. Tarahhomi, H. A. Rudbari, G. Bruno, *J. Mol. Struct.*, 1122 (2016) 123–133; (c) I. Kodrin, Ž. Soldin, C. Aakeröy, M. Đaković, *Cryst. Growth Des.* 16 (2016) 2040–2051.
- [31] (a) M. Sarkar, R. Clérac, C. Mathonière, N. G. R. Hearn, V. Bertolasi, D. Ray, *Inorg. Chem.*, 49 (2010) 6575–6585; (b) E. Lalinde, R. Lara, I. P. Lójepez, M. T. Moreno, E. Alfaro-Arnedo, J. G. Pichel, S. Piñero-Hermida, *Chem. Eur. J.*, 24 (2018) 2440–2456; (c) X. Zhu, P. Cui, S. Kilina, W. Sun, *Inorg. Chem.*, 56 (2017) 13715–13731.
- [32] Y. Zeng, X. Hu, F. Liu, X. Bu, *Chem. Soc. Rev.*, 38 (2009) 469–480.
- [33] (a) B. Bleaney, K. D. Bowers, *Proc. R. Soc. London, Ser. A*, 214 (1952) 451. (b) O. Kahn, *Molecular Magnetism*, VCH, Weinheim, (1993) 104.
- [34] N. F. Chilton, R. P. Anderson, L. D. Turner, A. Soncini, K. S. Murray, *J. Comput. Chem.* 34 (2013) 116–1175.
- [35] S. Jana, B. Shaw, P. Bhowmik, K. Harms, M. Drew, S. Chattopadhyay, S. Saha, *Inorg. Chem.*, 53 (2014) 8723–8734.

The formation of two new half condensed Schiff base complexes,  $[\text{CuL}(\mu\text{-}1,1\text{-N}_3)]_2$  (**1**) and  $[\text{CoL}_2]\text{N}_3\cdot\text{H}_2\text{O}$  (**2**) where  $\text{L} = (\text{E})\text{-}2\text{-}((2\text{-aminoethyl})\text{methyl})\text{-}4\text{-chlorophenol}$ , under the templating effect of a metal ion are reported. These new complexes have been structurally and analytically characterised. Complex **1** is an asymmetric  $\mu\text{-}1,1$  azide bridged dimer displaying weak antiferromagnetic interactions ( $J = -2.93 \pm 0.03 \text{ cm}^{-1}$ ), in agreement with the axial-equatorial  $\text{N}_3\text{-}$  linkage between the two copper centers. Complex **2** is a monomer of a low spin  $\text{Co(III)}$  ion. The examples provide a direction towards the deliberate synthesis of half condensed Schiff base complexes, whose structural and magnetic studies might be interesting for molecular magnetism studies.

